1

Working group report: QCD

Conveners: J. M. Campbell, K. Hatakeyama, J. Huston, F. Petriello

J. Andersen, R. Boughezal, M. Cooper-Sarkar, S. Dittmaier, G. Ferrera, S. Forte, T. Hapola, M. Grazzini, S. Höche, M. Klein, U. Klein, X. Liu, D. Kosower, K. Mishra, F. Piccinini, J. Rojo, J. Smillie

1.1 Introduction

A detailed understanding of quantum chromodynamics (QCD) phenomenology, both perturbative and non-perturbative, is crucial for a detailed understanding of physics at hadron-hadron, lepton-hadron, and lepton-lepton colliders. The QCD sub-group is somewhat different from most of the other sub-groups in the Snowmass workshop in that the emphasis is not on observables per se, but on the tools needed to understand the observables, in physics processes at all of the colliders mentioned above. There has been a great deal of progress in the last 5-10 years on QCD-related tools for calculation, simulation and analysis, at a level that would have been considered unlikely at best, if predicted at the time of the previous Snowmass workshop. Thus, it is our difficult task to summarize the level of the tools that exist now, to perform this extrapolation into the medium and long-term future, and to present a priority list as to the direction that the development of these tools should take. Most of our efforts concentrate on proton-proton colliders, at 14 TeV as planned for the next run of the LHC, and for 33 and 100 TeV, possible energies of the colliders that will be necessary to carry on the physics program started at 14 TeV. We also examine QCD predictions and measurements at lepton-lepton and lepton-hadron colliders, and in particular their ability to improve our knowledge of $\alpha_s(m_Z)$ (both) and our knowledge of PDFs (lepton-hadron colliders). Since the current world average of strong coupling measurements is dominated by the determinations made using lattice gauge theory we also explore possible improvements to our knowledge of $\alpha_s(m_Z)$ from such extractions.

It is useful to recall the basic structure of a parton-level cross section computed in perturbative QCD. The cross section can be written schematically as,

$$\sigma = \sum_{a,b} \int_0^1 \mathrm{d}x_1\, f_{a/A}(x_1,\mu_F^2) \int_0^1 \mathrm{d}x_2\, f_{b/B}(x_2,\mu_F^2) \Bigg\{ \int \mathrm{d}\hat{\sigma}_{ab}^{LO}\left(\alpha_s\right)\, \Theta_{\mathrm{obs}}^{(m)} + \alpha_s(\mu_R^2) \left[\int \left(\mathrm{d}\hat{\sigma}_{ab}^{V}\left(\alpha_s,\mu_R^2\right) + \mathrm{d}\hat{\sigma}_{ab}^{C}\left(\alpha_s,\mu_F^2\right) \right) \Theta_{\mathrm{obs}}^{(m)} + \int \mathrm{d}\hat{\sigma}_{ab}^{R}(\alpha_s)\, \Theta_{\mathrm{obs}}^{(m+1)} \right] \Bigg\} + \ldots \tag{1.1}$$

where we have sketched the terms that contribute up to the next-to-leading order (NLO) level in QCD. The first ingredients in the perturbative description are the parton distribution functions (pdfs), defined for a given species of parton a, b inside incoming hadrons A, B. The pdfs are functions of the parton momentum fractions x_1, x_2 and the factorisation scale μ_F. The leading order prediction depends on the hard matrix elements, contained in the factor $\mathrm{d}\hat{\sigma}_{ab}^{LO}$, which in turn depend on the value of the strong coupling, α_s, for strongly-interacting final states. In this equation the quantity α_s is a shorthand notation since it must be evaluated at the renormalization scale μ_R, $\alpha_s \equiv \alpha_s(\mu_R^2)$. Finally, the cross predicted cross section depends on the cuts that are applied to the m-parton configuration in order to define a suitable observable, $\Theta_{\mathrm{obs}}^{(m)}$. In the case of cross sections for multi-jet processes this factor accounts for the jet definition that is

required for infrared safety. At NLO there are further contributions, as indicated on the second line of the equation. The virtual diagrams contain an explicit dependence on the renormalization scale, $\mathrm{d}\hat{\sigma}^V_{ab}\left(\alpha_s, \mu_R^2\right)$ while the collinear counterterms that are necessary in order to provide an order-by-order definition of the pdfs introduce explicit factorization scale dependence, $\mathrm{d}\hat{\sigma}^C_{ab}\left(\alpha_s, \mu_F^2\right)$. The effects of real radiation, $\mathrm{d}\hat{\sigma}^R_{ab}(\alpha_s)$ now include a cut on the $(m+1)$-parton configuration. They may therefore be sensitive to kinematic effects that are not present in the m-parton case, for instance the effect of jet vetoes in electroweak processes. At next-to-next-to-leading order (NNLO) we would include terms in equation 1.1 that have an explicit factor of $\alpha_s(\mu_R^2)$ in addition to those present at leading order. In outline the extension is clear, with the introduction of configurations that contain m, $m+1$ and $m+2$ parton. As a result NNLO calculations may be even more sensitive to kinematic effects that are only approximately modelled, if at all, in lower orders. However the interplay between soft and collinear divergences in each of these contributions greatly complicates the calculation of NNLO effects.

From this guiding equation it is clear that detailed QCD predictions require knowledge of:

- parton distribution functions (PDFs) and their uncertainties
- $\alpha_s(m_Z)$ and its uncertainty
- higher order corrections to cross sections
- the impacts of restrictions in phase space, such as jet vetoes

Measurements at 14 TeV and higher will access a wide kinematic range, where PDF uncertainties and the impact of higher order corrections may be large. At scales large compared to the W mass, electroweak (EWK) corrections can be as important as those from higher order QCD; mixed QCD-EWK corrections also gain in importance. Higher energies also imply higher luminosities, which require the ability to isolate the physics of interest from the background of multiple interactions accompanying the higher luminosities. Much of the physics of interest will still involve the production of leptons, jets, etc at relatively low scales; as the center-of-mass energy increases, both the perturbative and non-perturbative environments may make precision measurements of such objects more difficult.

In this contribution, we cannot hope for a comprehensive treatment of all of the above, but will try to summarize the most important aspects of QCD for future colliders.

1.2 Parton density functions

Parton distributions are an essential ingredient of present and future phenomenology at hadron colliders [1, 2, 3]. They are one of the dominant theoretical uncertainties for the characterization of the newly discovered Higgs-like boson at the LHC, they substantially affect the reach of searches for new physics at high final state masses and they limit the accuracy to which precision electroweak observables, like the W boson mass or the effective lepton mixing angle, can be extracted from LHC data [4].

1.2.1 Current knowledge and uncertainties

The determination of the parton distribution functions of the proton from a wide variety of experimental data has been the subject of intense activity in the last years. Various collaborations provide regular updates

of their PDF sets. The latest releases from each group are ABM11 [5], CT10 [6], HERAPDF1.5 [7, 8], MSTW08 [9] and NNPDF2.3 [10]. A recent benchmark comparison of the most updated NNLO PDF sets was performed in Ref. [11], where similarities and differences between these five PDF sets above were discussed, and where W, Z and jet production data was used to quantify the level of agreement of the various PDF sets with the Tevatron and LHC measurements.

A snapshot of the comparisons between recent NNLO PDFs at the level of parton luminosities and cross section can be seen in Fig. 1-1, where we compare the gluon-gluon PDF luminosities between the five sets. We also show the predictions for Higgs production cross section in the gluon-fusion channel and in WH associated production.[1] Results have been computed using the settings discussed in Ref. [11].

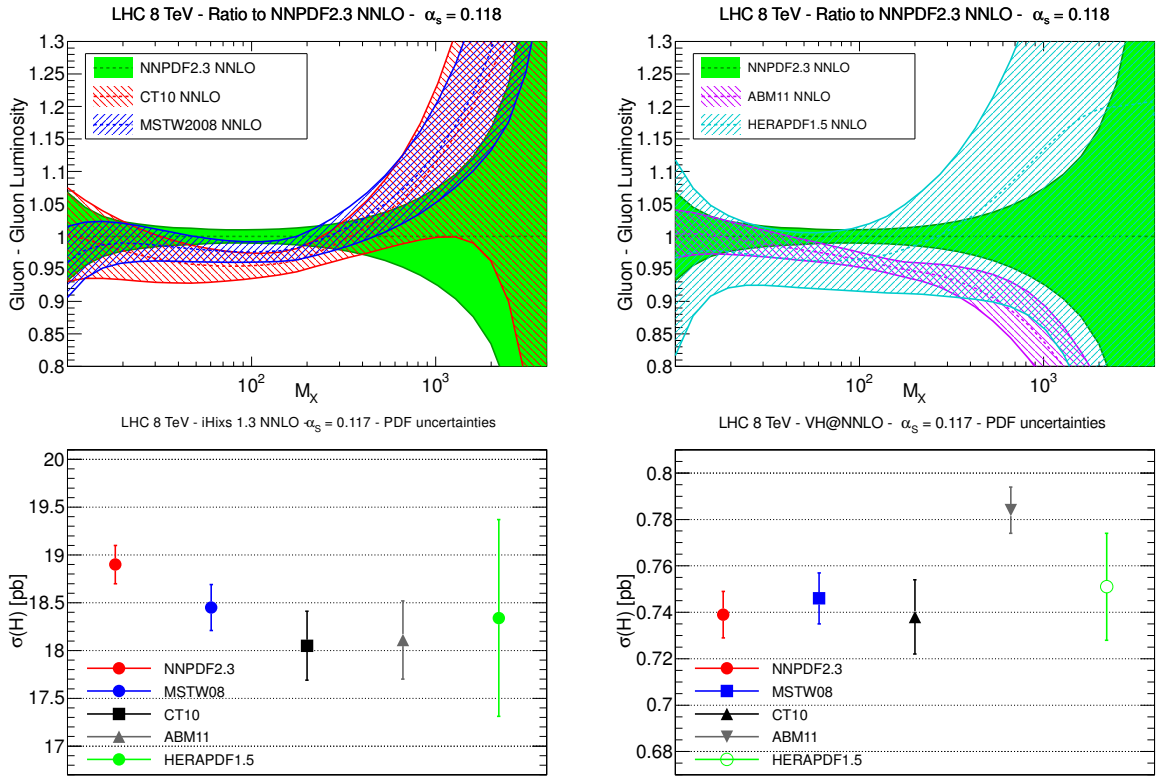

Figure 1-1. *Upper plots: Comparison of the gluon-gluon luminosity at the LHC 8 TeV as a function of the final state mass M_X between the ABM11, CT10, HERAPDF1.5, MSTW and NNPDF2.3 NNLO PDF sets. Lower plots: predictions for the Higgs production cross sections at LHC 8 TeV for the same PDF sets, in the gluon-fusion channel (left plot) and in the WH channel (right plot).*

As compared to previous comparisons, one of the main conclusions of the benchmark study [11] was that the agreement between the three global PDF sets, CT, MSTW and NNPDF has improved for most PDFs and ranges of Bjorken-x. On the other hand, there are still important differences that need to be understood, and that have substantial phenomenological impact. To begin with, the gluon luminosity for the three PDF

[1] An extensive set of comparison plots for PDFs, parton luminosities, LHC total cross sections and differential distributions at NLO and NNLO and for different values of $\alpha_s(M_Z)$ can be found in
. `https://nnpdf.hepforge.org/html/pdfbench/catalog/`

sets differs maximally for $m_X \sim 125$ GeV, as can be seen from Fig. 1-1, and it would be important to understand the source of these differences to improve the agreement of the three sets for the gluon-induced Higgs production cross sections. In addition, very large PDF uncertainties affect the production of heavy massive particles, in the TeV range, where also central values can be quite different. These large uncertainties at large masses degrade the prospects for eventual characterization of new BSM heavy particles. On top of this, there are theoretical uncertainties due to the choice of heavy quark GM-VFN scheme, specific choices in the fitted dataset and methodological differences that still require further understanding to improve the agreement between the various PDF sets.

In the next subsection we discuss what are the prospects to obtain further constraints in PDFs from LHC data.

1.2.2 Parton distributions with QED corrections

Precision predictions for electroweak processes at hadron colliders require not only (N)NLO QCD corrections, but also the consistent inclusion of QED corrections on parton distribiutions and photon-initiated contributions. QED and electroweak corrections for various relevant collider processes have been computed in the last years in processes like inclusive W, Z production, vector boson pair production, $t\bar{t}$ and dijet production among many others. On the other hand, it is also known that a fully consistent treatment of electroweak corrections requires the use of parton distributions that in turn incorporate QED effects as well. QED effects to parton distributions have two main implications: first of all, the standard QCD DGLAP evolution equations are affected by $\mathcal{O}(\alpha)$ corrections and the associate breaking of isospin invariance, and, phenomenologucally more important, the photon PDF needs to the determined from experimental data just as the quark and gluon PDFs.

Until recently, a single PDF set with QED corrections was available, the MRST2004QED set [25], where the photon PDF was determined based on a model assumptions. However, now the NNPDF framework has also been extended to provide PDF sets with QED corrections, and NNPDF2.3 QED is already available in the NNPDF `HepForge` website.[2] NNPDF2.3 QED avoids any model assumption on the photon PDF and derives $\gamma(x, Q^2)$ and its associated uncertainties from a global fit to DIS and LHC data, where in the latter case neutral current and charged current vector boson production data provide stringent constraints on the shape and normalization of $\gamma(x, Q^2)$.[3]

Electroweak corrections to parton distribution functions have important phenomenological implications, in particular for the electroweak production of high invariant mass final states. These include the measurement of the W mass, searches for W' and Z' resonances in the tails of the W and Z distributions and vector boson pair production among many others. The main effect is that the substantial uncertainties on the large-x photon PDF (that stem from the lack of available experimental constraints) translates into very large uncertainties from photon-initiated contributions, that can be as large as a factor 100%.

As an illustration of these phenomenological consequences, in Fig. 1-2 we have computed the predictions of the NNPDF2.3 QED set for WW production at the LHC for various center of mass energies, compared with the results of the reference NNPDF2.3 set, as well as with the predictions from MRST2004QED. The computation has done at leading order in the electroweak coupling but including photon-initiated diagrams, using the same settings as in Ref. [28]. We show the total cross section as a function of the cut in the $M_{\rm WW}$

[2] `https://nnpdf.hepforge.org/html/nnpdf23qed/nnpdf23qed.html`

[3] Preliminary results with the NNPDF2.3 QED set have been presented in Refs. [26, 27], a more detailed paper is in preparation.

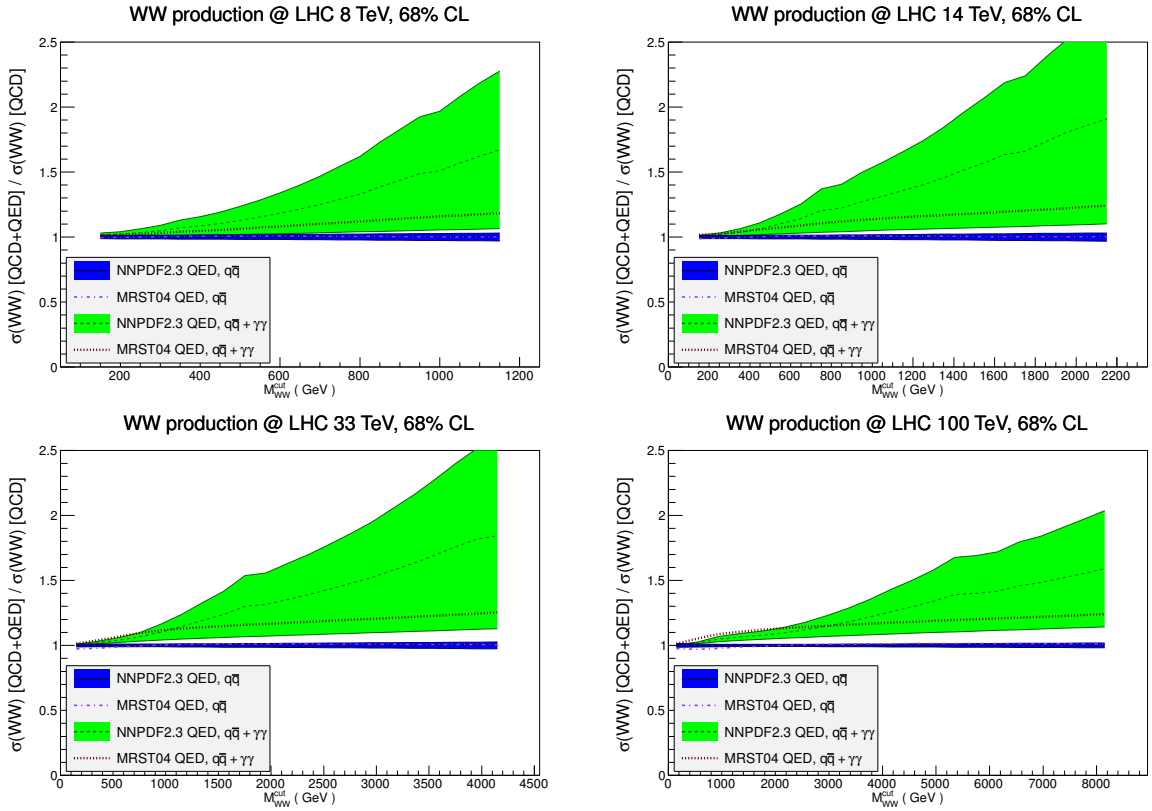

Figure 1-2. *The predictions of the NNPDF2.3 QED set for WW production at the LHC for various center of mass energies, compared with the results of the reference NNPDF2.3 set, as well as with the predictions from MRST2004QED. We show the total cross section as a function of the cut in the $M_{\rm WW}$ invariant mass, for 8, 14, 33 and 100 TeV energies. See text for more details.*

invariant mass, for 8, 14, 33 and 100 TeV energies.[4] Is clear that the QED-induced theoretical uncertainties are substantial and that do degrade the constraining power of BSM searches in this channel, for instance heavy resonances that decay in WW pairs, and that these effects are more severe the higher the cut in the invariant mass of the WW pair. Of course, as the energy is increased, for a given value of M_{WW} the PDF uncertainties decrease, but they are still very substantial at the highest available masses in each case, a factor 2 at least.

In summary, the development of parton distributions with QED corrections is an important ingredient of fully consistent theoretical predictions of hadron collider processes that include both higher order corrections in the QCD and EW couplings. On the other hand, the same analysis reveal the urgent need for more experimental data to constrain the photon PDF $\gamma(x, Q^2)$, and thus to reduce the currently large QED-induced uncertainties that affect high mass electroweak production at the LHC.

[4] We thank T. Kasprick for providing us with these results.

1.2.3 PDF constraints from future LHC data

The excellent performance of the Large Hadron Collider is substantially increasing the range of processes that can be used to constrain PDFs in a global analysis. Let's begin with the traditional processes at hadron colliders that have been used PDF constraints, namely inclusive jets and W, Z production. Inclusive jet and dijet data are now available up to the TeV region from ATLAS and CMS [12, 13], and provide important constrains on the poorly known large-x quarks and gluons. In addition, ATLAS has presented the measurement the ratio of inclusive jet cross sections between 2.76 TeV and 7 TeV [14]. Such ratios between different center of mass energies [15] increase the PDF sensitivity of data taken at a single energy, since on the one hand many experimental uncertainties cancel in a dedicated measurement of a cross section ratio, and on the other hand several theory systematics, like scale variatios, cancel as well. Future data at 14 TeV and with increased luminosity will allow to pin down quark and gluon PDFs up to very large values of x, providing in turn crucial input for BSM high mass particle production. In this respect, recent progress towards the full NNLO QCD corrections for inclusive and dijet production [16] should make feasible to achieve a per-cent accuracy on these observables by the time of the 13 TeV data taking.

The precision measurements of W and Z boson production at hadron colliders provide important information on quark flavor separation, and on top allow to reduce systematic uncertainties of important observables like the W boson mass [4]. While the Z rapidity distribution and the W lepton asymmetry from the tevatron and the LHC have been by now available for some time, recently the range of available processes has been extended by the measurement of the off-peak neutral current Drell-Yan process by ATLAS, CMS and LHCb. Such measurements provide useful information on the large-x quarks and antiquarks (for high mass) and in the small-x gluon and possible departures from lineal DGLAP evolution, in the case of low mass DY, where particularly striking signatures ave been predicted for the LHCb kinematics. In this respect, future measurements at higher energies will benefit on the one hand an increased coverage in the dilepton invariant mass (in the case of neutral current scattering) allowing to probe very large-x antiquarks, which are effected by very large PDF uncertainties, while on the other hand the measurements in the peak region will benefit from reduced systematics and by negligible statistical uncertainties.

On top of the traditional processes discussed above, many new collider observables have recently become available for the first time for their use in PDF fits. The recent calculation of the full NNLO top quark production [17] cross section makes possible for the first time to include top quark data into a NNLO analysis to constrain the large-x gluon PDF [18]. This is an important results since top production is currently the only hadronic observable which is both directly sensitive to the gluon and can be included in a NNLO global fit without any approximation. In turn, the more accurate gluon PDF translates into an improvement of the theory predictions for various high-mass BSM processes driven by the gluon luminosity.

Another interesting result of Ref. [18] is that the gluon determined from a NNPDF2.1 fit to inclusive DIS HERA data only [19, 20] and supplemented by LHC top production data is quite close to that of the global fit, driven by jet data, a remarkable consistency test of the global QCD analysis framework. Future precision measurements of differential distributions in top quark pair production will allow to enlarge the range of Bjorken-x where the gluon PDF is being probed, specially once the NNLO calculation of [17] is extended to the fully differential case. In addition to top quark data, the use of LHC isolated photon data and photon+jet data has also been advocated in order to pin down the gluon PDF [21, 22], though this process is affect by missing higher order and non perturbative uncertainties.

Turning to the constraints on the quark sector, the production of W and Z bosons in association with jets, for high p_T values of the electroweak boson, is a clean probe at the LHC of both quark flavor separation and of the gluon PDF [23]. In particular, ratios of W and Z distributions at large p_T provide constrains on quarks and antiquarks while benefiting from substantial cancellations of experimental and theory uncertainties. This

is a good example of a process currently limited by statistics, and that with future LHC data will benefit of a much increased constraining power. Another important source of information is on the quark PDFs is W production in association with charm, directly sensitive to the strange PDF [24], the worst known of all light quark flavors. Preliminary results for this important process has been recently measured by both ATLAS and CMS. Interestingly, the two measurements seem to pull in different directions for the strange PDF, with CMS showing good agreement with the strangeness suppression of global PDF fits derived from the neutrino DIS charm production data, while ATLAS prefers a symmetric strange sea, similar as previously derived from their inclusive W and Z data. Including all these datasets into the global PDF fits would then be crucial to determine the optimal strange PDF which accounts for all experimental constraints.

Putting everything together, is clear that the LHC will provide in the next years a plethora of new measurements that will be used to improve our knowledge of parton distributions. Quantitative projections in this respect are difficult since precision measurements, like those used in PDF analysis, are dominated by systematics, which are notoriously difficult to predict. In addition, correcting for pile-up in the high-luminosity phase of the LHC might render even more complicated such analysis. But all in all, there are good prospects that in the next years PDFs will be determined with increasingly better accuracy, in turn improving the theory predictions for Higgs boson characterization and New Physics searches.

1.2.4 Luminosities and uncertainties for 14, 33 and 100 TeV

As discussed above, in order to assess similarities and differences between PDF sets, it is useful to compare parton luminosities for different channels as a function of the final state mass M_X of the produced system, for different values of the hadronic collider energy. In the following we will redo the comparisons presented in Ref. [11], but this time for higher energy incarnations of the LHC, at 14 TeV, 33 TeV and 100 TeV. This comparison is shown in Fig. 1-3, where we compare the quark-quark, quark-antiquark and gluon-gluon luminosities between the most updated CT, MSTW and NNPDF NNLO PDF sets at these three center of mass energies.

While in general we observe reasonable agreement between the three sets, there are also some cases where the agreement is marginal, like for the gluon-gluon luminosity, or even non existing, like the very high mass range for the quark-quark luminosity at 100 TeV. As well known, for fixed value of M_X increasing the collider center of mass energy results in a reduction of PDF uncertainties, since the smaller ratio $M_X/\sqrt{s}$ implies that PDFs at smaller values of Bjorken-x are begin probed, which are better constrained by existing data.

1.2.5 Improvements from LHeC

1.3 The strong coupling

1.4 Higher-order corrections

The current standard for most theoretical predictions at hadron colliders is NLO, with a small number of calculations extended beyond this to NNLO. In this section we review the behavior of some these predictions for LHC operations at 14 TeV and for proton-proton collisions at 33 and 100 TeV. We also summarize recent

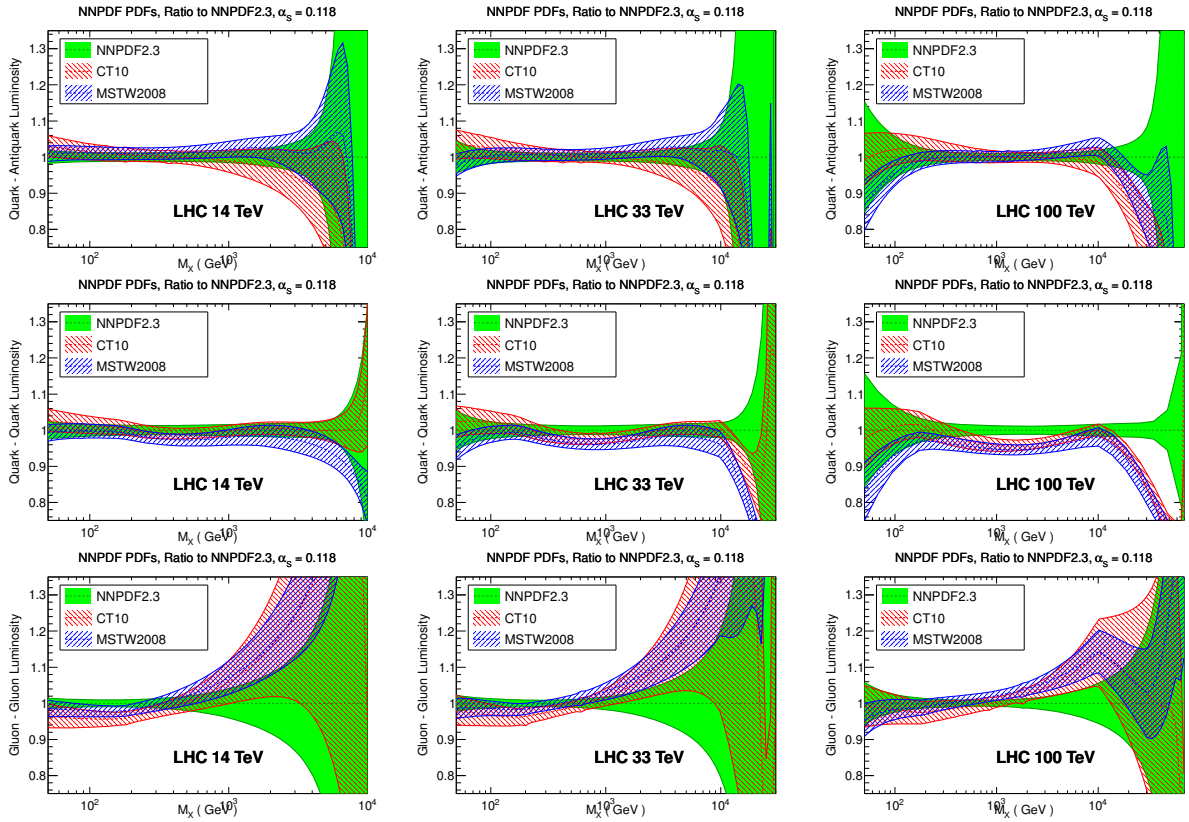

Figure 1-3. *Comparison of the partonic luminosities at 14, 33 and 100 TeV between the CT10, MSTW and NNPDF2.3 NNLO PDF sets. From top to bottom: quark-antiquark luminosity, quark-quark luminosity, and the gluon-gluon luminosity.*

results on extending the predictions for one of the most important cross sections, Higgs boson production by gluon fusion, to N^{3}LO. We also provide an overview of the highest-priority perturbative calculations, ones that could feasibily be tackled in the next 5–10 years.

1.4.1 NLO cross sections at 14, 33 and 100 TeV

As a first step towards investigating the physics potential of future proton-proton colliders, it is interesting to investigate the center-of-mass energy dependence of notable cross-sections at such machines. Figure 1-4 shows the predicted cross sections for a selection of basic processes, ranging over twelve orders of magnitude from the total inelastic proton-proton cross section to Higgs boson pair-production. For inclusive jet and direct photon production, 50 GeV transverse momentum cuts are applied to the jet and the photon respectively. The cross sections presented in this figure have been calculated at next-to-leading order in QCD using the MCFM program [31], or taken from the European Strategy report [60] (in the case of Higgs cross sections).

The growth of the cross-sections with $\sqrt{s}$ largely reflects the behavior of the underlying partonic luminosities. For instance, the top pair cross section is dominated by the partonic process $gg \to t\bar{t}$ and the gluon-gluon luminosity rises significantly at higher values of $\sqrt{s}$. The same holds true for the Higgs production channel

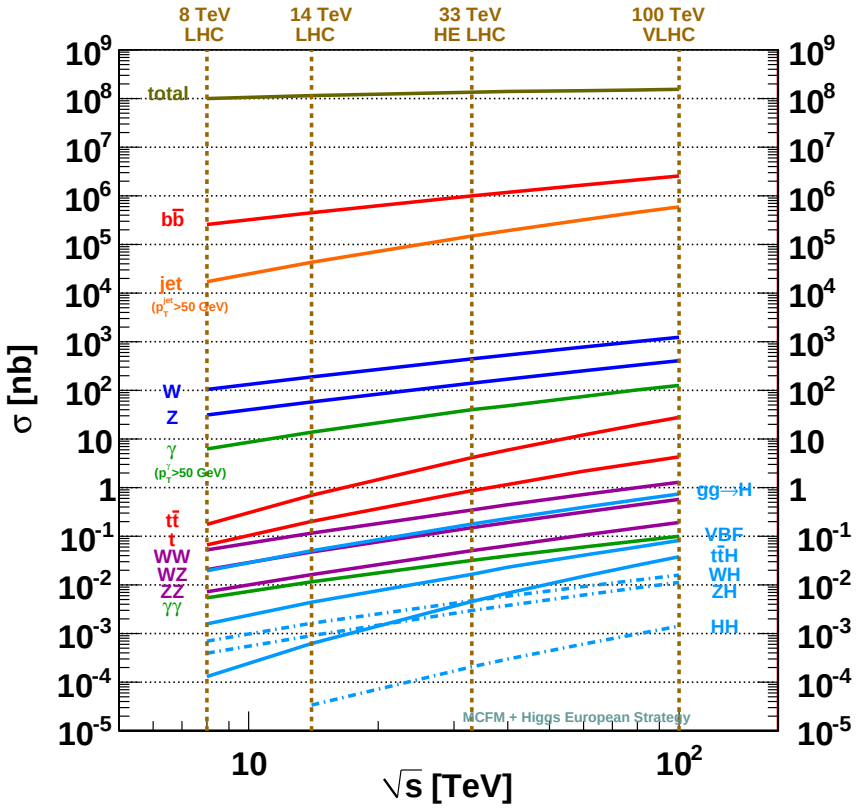

Figure 1-4. *Cross section predictions at proton-proton colliders as a function of center-of-mass operating energy, $\sqrt{s}$.*

$t\bar{t}H$ but, in contrast, the associated production channels are dominated by quark-antiquark contributions and rise much more slowly. The different behavior means that, unlike at current LHC operating energies, the $t\bar{t}H$ channel becomes the third-largest Higgs production cross section at 33 TeV and above. As a figure of merit for estimating the difficulty of observing the Higgs pair production process it is not unreasonable to consider the ratio of its cross section to the top pair cross section. For instance, for many of the possible Higgs boson decays the final states could receive significant background contributions from the top pair process. The fact that both processes are predominantly gluon-gluon induced means that this measure is approximately constant across the range of energies considered. It is therefore not clear that the prospects for extracting essential information from the Higgs-pair process would be significantly easier at a higher-energy hadron-collider.

A different sort of contribution to event rates can also be estimated from this figure. The contribution of double parton scattering (DPS) – where a single proton-proton collision is responsible for two hard events – can be estimated by,

$$\sigma_{XY}^{\mathrm{DPS}} \approx \frac{\sigma_X \sigma_Y}{15\ \mathrm{mb}}\ . \tag{1.2}$$

In this equation the DPS contribution for the final state XY is related to the usual cross sections for individually producing final states X and Y using the effective DPS cross section. This cross section appears

to be approximately independent of energy up to 8 TeV and is approximately 15 mb (for example, see Ref. [32] for a recent measurement at 7 TeV). Of course the uncertainty on the effective cross section, and indeed on the accuracy of equation (1.2) itself, is such that this should be considered an order-of-magnitude estimate only. A particularly simple application of this is estimating the fraction of events for a given final state in which there is an additional DPS contribution containing a pair of b-quarks. This fraction is clearly given by the ratio, $\sigma_{b\bar{b}}/(15\text{ mb})$. From the figure this fraction ranges from a manageably-small 2% effect at 8 TeV to a much more significant 20% at 100 TeV. More study would clearly be required in order to obtain a true estimate of the impact of such events on the physics that could be studied at higher energies, but these simplified arguments can at least give some idea of the potentially troublesome issues.

As an example of the behavior of less-inclusive cross sections at higher energies, Figure 1-5 shows predictions for $H + n$ jets $+ X$ cross sections at various values of $\sqrt{s}$ and as a function of the minimum jet transverse momentum. The cross sections are all normalized to the inclusive Higgs production cross section, so that the plots indicate the fraction of Higgs events that contain at least the given number of jets. The inclusive Higgs cross section includes NNLO QCD corrections, while the 1- and 2-jet rates are computed at NLO in QCD.

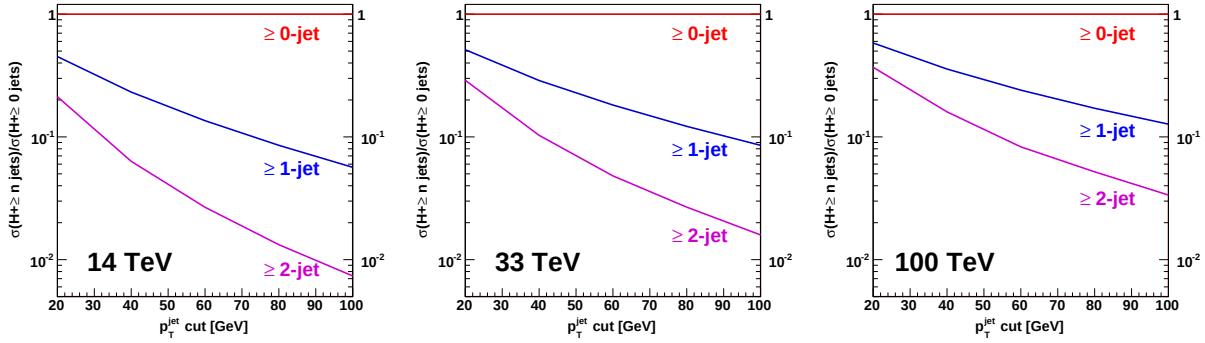

Figure 1-5. *Cross sections for the production of a Higgs boson produced in association with n or more jets, for $n = 0, 1, 2$, normalized to the inclusive Higgs cross section ($n = 0$). Cross sections are shown as a function of the minimum jet p_T and are displayed for a proton-proton collider operating at 14 TeV (left), 33 TeV (center) and 100 TeV (right).*

The extent to which additional jets are expected in Higgs events is clearly strongly dependent on how the jet cuts must scale with the machine operating energy. For instance, consider a jet cut of 40 GeV at 14 TeV, a value in line with current analysis projections. For this cut, approximately 20% of all Higgs boson events produced through gluon fusion should contain at least one jet and the fraction with two or more jets is expected to be around 5%. To retain approximately the same jet compositions at 33 and 100 TeV requires only a modest increase in the jet cut to 60 and 80 GeV respectively.

At higher operating energies it is especially interesting to compare predictions produced using the standard perturbative expansion, here at NLO, with alternative formalisms that directly appeal to the high energy limit. One such formalism is encoded in the program HEJ ("High Energy Jets") [57, 58] that implements a resummation scheme based on the factorisation of scattering amplitudes in the high energy limit. For this study we investigate predictions for $H + 2$ jet events, with particular interest in the region where two of the jets are separated by a large rapidity span. As well as being relevant for separating the gluon fusion and vector boson fusion processes, this region is expected to be particularly sensitive to differences between the predictions of NLO QCD and HEJ [61]. Jets are reconstructed using the k_T algorithm with $D = 0.6$ and

$|y| < 5$. In the first scenario we consider a minimum transverse momentum cut of 40 GeV for operating energies of 14, 33 and 100 TeV. In the second scenario the jet cut is doubled to 80 GeV at 33 TeV and again to 160 GeV at 100 TeV.

The results of this study are shown in Figure 1-6. Predictions are shown for the ratio of 3-jet to 2-jet events, as a function of the rapidity difference between the two most widely-separated jets. The uncertainty band is obtained by varying the scale choice by a factor of two about the central value ($H_T/2$, where H_T is the sum of the total transverse momentum of all objects in the final state, for MCFM).

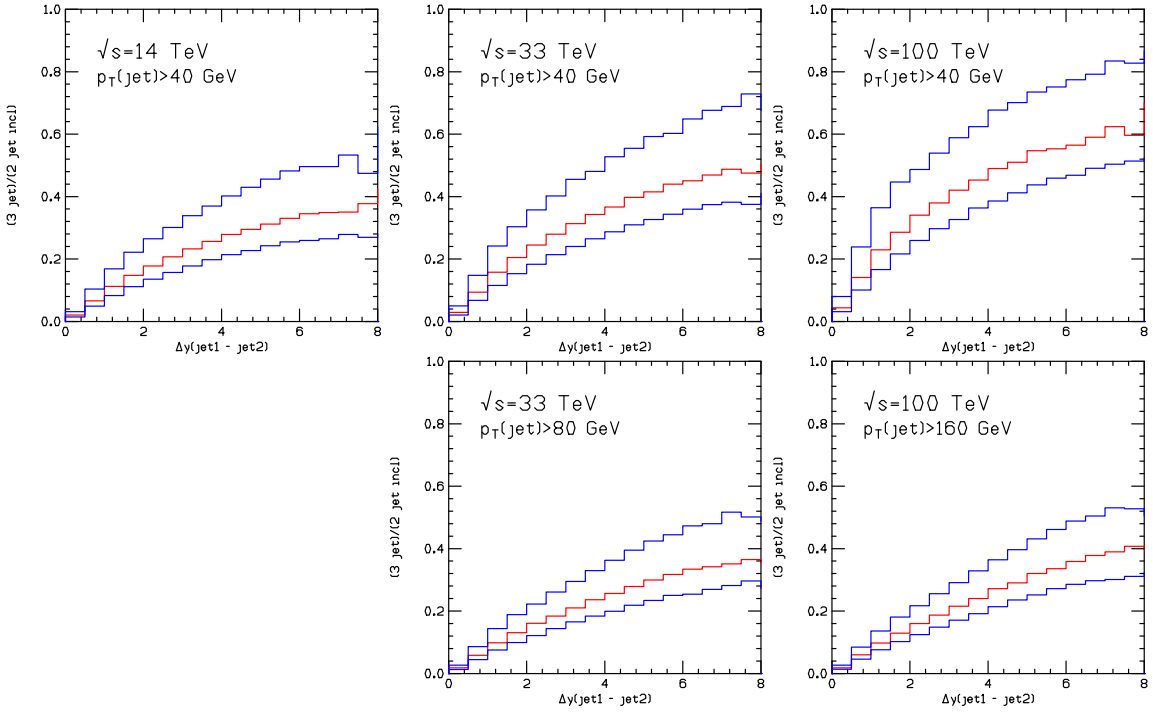

Figure 1-6. *The ratio of number of events that contain at least three jets to the number that contain two jets, as a function of the rapidity difference between the two most widely-separated jets. Predictions are obtained using the NLO calculation of the $H + 2$ jet process and are shown at three operating energies. The jet transverse momentum cut is at 40 GeV (top), or scales with the operating energy (bottom).*

1.4.2 Extrapolation from existing NLO results

The progress within the last 5 years in the calculation of NLO corrections for complex final states has been truly impressive, as witnessed for example by the calculation of $W + 5$ jets by the Blackhat+Sherpa collaboration [62]. Of course, there is a limit, as increasing the number of partons in the final state by definition increases the complexity of the calculation, while the physics reward (typically) decreases. Within a matrix-element + parton shower framework, additional jets can be added either at leading order or through the parton shower. In addition, there are heuristic tools that can be developed to extrapolate cross sections for higher jet multiplicity based on the patterns observed at lower jet multiplicity. For instance, known results for $W + 2$ through $W + 5$ jet production can be used to assess the scaling behavior of the $W + n$ jet

cross sections [5] Defining the quantity $R^{\pm} = \sigma(W^{\pm} + n \text{ jets})/\sigma(W^{\pm} + n - 1 \text{ jets})$, Blackhat+Sherpa have developed predictions for this ratio for $n > 3$, in pp collisions at 7 TeV, for jets with $p_T > 25$ GeV. The predictions are:

$$R^{+}_{\text{NLO}} = 0.0263 \pm 0.009 - (0.009 \pm 0.003)$$
$$R^{-}_{\text{NLO}} = 0.0248 \pm 0.008 - (0.009 \pm 0.002)$$

From these formulae, the cross sections at NLO for $W + 6$ or 7 jets can be predicted, without any actual calculation. Of course, such scaling formulae are strongly dependent on the kinematic regions being considered, but can easily be re-assessed for different cuts or center-of-mass energies.

1.4.3 Computational complexity

The advances of NLO and NNLO multi-leg calculations have resulted in programs that are (1) very complex and (2) very time-consuming to run using the resources available to a typical user. It can thus be difficult for a full dissemination of the theoretical results to the experimental community. The Blackhat+Sherpa collaboration has partially addressed these issues by releasing results for $W/Z + n$ jets in ROOT ntuple format, with all information needed for calculation of physical cross sections with a variety of jet parameters and cuts. In addition, the results can be re-weighted for different scales and different PDFs. The cost is the presence of very large outputs, but subdivided into files of a few GB that are ideal for parallel processing. Ntuples are probably not practical, though, for some of the more complex NNLO calculations, such as inclusive jet production, where the number of files needed would be prohibitive. Making the resultant program user-friendly, though, can take a great deal of time.

An alternative is to make such complex programs available to the user on high performance computing platforms, which inherently have much greater processing and storage capabilities; in addition, the programs may be pre-compiled by the authors insuring that the calculation is run correctly. Initial tests of HPC platforms have been successfully carried out during the Snowmass workshop. We have shown weak scaling up to 16000 cores on IBM BlueGene/Q, up to 8192 cores on CRAY XK7, and strong scaling up to 1024 cores on CRAY XK7 using Sherpa. Another possibility for large-scale production runs may be the Open Science Grid. The first attempt to introduce it to the pQCD community may have failed, but it has great potential to harvest existing resources.

1.4.4 Improvements to parton showers

General-purpose event generators have been undergoing tremendous development over the past years. Both the fixed-order and logarithmic accuracy underpinning their simulations of perturbative QCD have been improved in order to match increased precision needs in the experiments.

The basis for the these developments was established by the MC@NLO technique [39], which matches NLO QCD calculations to parton showers, such that fully differential events can be generated at the particle level. The POWHEG [40, 41] method was later introduced to eliminate negative weights from simulations.

Parton-shower matched predictions have been provided for some of the most challenging NLO calculations to date, including, for example, $pp \to W + 3$ jets [49] and $pp \to t\bar{t}$+jet [50]. The current limitation in matching

[5] $W + 1$ jet behaves differently because of missing production channels and kinematic differences.

to even higher multiplicity processes is not of algorithmic nature, but purely computational, and it is related to the memory consumption of executables. Fixed-order calculations benefit from the fact that they can be split into different parts, corresponding to Born, virtual correction, integrated infrared subtractions and real-emission correction minus real subtraction. Due to the intricate interplay between real and virtual corrections in MC@NLO and POWHEG, such a splitting is harder to achieve when matching to a parton shower.

Different proposals were made to combine MC@NLO simulations of varying jet multiplicity into inclusive event samples [42, 43]. They are natural extensions of the CKKW(-L) [44, 45] and MLM [46] leading-order merging schemes to the next-to-leading order, respectively. Another, entirely independent method was introduced earlier, which relies on a different subtraction scheme [47, 48]. The simulations provided by these new techniques can be used to obtain NLO-accurate predictions for different jet multiplicities at the same time.

Achieving this level of fixed-order accuracy has been a priority in the development of Monte-Carlo event generators for more than a decade. The current technology has undoubtedly benefited greatly from the advances in computing fixed-order NLO QCD corrections at large jet multiplicity in a fully automated manner. These calculations provide the parton-level input for the new merging methods.

NLO-merged predictions have been provided for $pp \to W/Z$+jets with up to two jets described at NLO accuracy [42], $pp \to H$+jets in gluon fusion, with up to one jet at NLO accuracy [48, 43] and $pp \to t\bar{t}$+jets with up to one jet at NLO accuracy [43, 51]. All related implementations are fully automated and can, in principle, be used for any type of reaction. However, because MC@NLO parton-level predictions are needed as an input, the current limitations are identical to those for MC@NLO. They are not due to algorithmic deficiencies, but mostly due to memory constraints on production systems and restrict the usage of the methods to processes with fewer than four light jets in the final state computed at NLO.

It is conceivable that working techniques for matching NNLO fixed-order calculations to parton-shower simulations will be constructed in the near to mid-term future. Such a matching, which could be dubbed 'MC@NNLO', would further stabilize predictions for the differential cross section at lowest multiplicity, and eliminate the unitarity violation observed in most NLO merging methods in a natural way.

An alternative technique already exists, which does not rely on a modified subtraction scheme to construct counterterms for fixed-order calculations, but on constructing counterterms for the parton shower, at the order at which the shower is to be matched [47]. This is very easy to achieve. The method has been used as proof of principle to provide NNLO matched predictions for e^+e^- →jets production [47].

At the same time that matching to fixed-order NNLO calculations is being developed, the logarithmic accuracy of parton shower simulations must be improved systematically, in order not to degrade the precision of the fixed-order result after matching. This involves two developments:

Firstly, corrections which are sub-leading in the number of colors, N_c, must be included. A proposal to do this was formulated some time ago [52], but first steps to implementation were taken only recently [53, 54]. The importance of sub-leading N_c corrections in processes with non-trivial color structure at Born level was observed in an analysis of the $t\bar{t}$ forward-backward asymmetry [51]. Respecting the full color structure during parton evolution will allow to include all next-to-leading logarithmic effects in the parton shower, in a manner that is independent of the actual evolution variable, and therefore does not rely on angular ordering.

Secondly, it will be beneficial to systematically extend parton-showers to higher logarithmic accuracy, for example by including higher-point splitting functions. An alternative approach, based on the matching of parton showers to analytic calculations at higher logarithmic accuracy also seems promising. Such an

approach was used already to generate predictions for the thrust distribution and several event shapes in e^+e^- →jets [55]. First results for $pp \to e^+e^-$ have been reported [56].

Logarithmic enhancements of the cross section at high energy, which are resummed in the HEJ framework [57, 58] could be crucial to understanding the structure of multi-jet events at the LHC. Including these contributions in event generators may become important [59].

1.4.5 A study of perturbative stability: WH production at NNLO

Sometimes it is experimentally necessary to require an exclusive final state, for example by restricting the number of jets allowed to be present. This is true for some current LHC analyses and will no doubt continue to be true for higher energies. This requirement of an exclusive final state can result in the presence of large logarithms due to the unbalancing of the cancellation between positive real emission terms and negative virtual corrections, thus affecting the convergence and reliability of the perturbative series. As an example, consider searches for Higgs boson production in the associated mode (VH). While this has been the major Higgs boson search channel at the Tevatron, at the LHC it suffers from large backgrounds. A precise measurement in this channel (with the Higgs decaying into a $b\bar{b}$ pair) can still be very useful in the years following the Higgs boson discovery in order to understand the Higgs coupling to b-quarks. A relative reduction in the background at the LHC can be achieved by requiring the vector boson and the Higgs boson to be at large transverse momentum, with no additional jets present greater than some threshold. While the impact of higher order QCD corrections is mild for the inclusive measurement, such restrictions can greatly affect the size of the higher order corrections and thus the convergence of the perturbative series. In this context, the issue was first raised in the original exclusive NNLO calculation of WH production [29].

In this report we address the extent to which this issue is exacerbated in predictions for higher energy proton-proton colliders. For the following study the transverse momentum of the W boson is required to be greater than 200 GeV. The Higgs boson decays into a $b\bar{b}$ pair that is reconstructed as a "fat jet" using the Cambridge-Aachen algorithm with $R = 1.2$. This fat jet must also be at large transverse momentum, greater than 200 GeV. In addition to these cuts, any additional jets were required have transverse momenta below 40 GeV. The study was repeated at 14, 33 and 100 TeV, with the results shown in Figure 1-7 (left). The cross section is plotted as a function of the transverse momentum of the fat (Higgs) jet. As the center-of-mass energy increases, the effect of such stringent cuts increases. There are large negative corrections when going from LO to NLO, resulting in a NLO K-factor (NLO/LO) as low as 0.3 (for 100 TeV). The corrections from NLO to NNLO by comparison are modest, but the strong reduction from LO to NLO indicates that the fixed order prediction may be unreliable, and a resummed cross section is necessary to achieve a reliable prediction. As alternative scenarios at higher energies, Figure 1-7 (right) shows the effect of raising the jet threshold to 60 GeV (at 33 TeV) and 80 GeV (at 100 TeV). In these cases, the effect of allowing additional phase space results in a better-behaved perturbative series, and cross sections that behave order-by-order in a manner that is more similar to the pattern observed for a 40 GeV veto at 14 TeV.

1.4.6 Beyond NNLO: Higgs boson production

Small x "BFKL" (or high-energy) resummation and large x "Sudakov" (or threshold, or soft-gluon) resummation provide information on the all-order behaviour of a wide class of hadron collider observables in two opposite kinematic limits. Because the Mellin transform of a partonic cross section $\sigma(N, \alpha_s(M^2))$ is an analytic function of the variable N which is conjugate to the longitudinal momentum scaling variable (usually

called x or τ), this information provides powerful constraints on the unknown higher order perturbative corrections to the cross-section.

The use of resummation to determine approximate higher order perturbative corrections has a long history, and, in particular, approximate NNLO jet cross sections determined using results from threshold resummation [38] are routinely used in PDF fits. Recently, in Ref. [33] it was suggested that especially accurate results can be obtained if maximal use is made of analyticity constraints, by not only combining information from differenmt kinds of resummation, but also making sure that the known all-order analytic properties of the cross section are reproduced as much as possible. So, for instance, while as $N \to \infty$ $\sigma(N, \alpha_s(M^2)) \sim \sum_k (\alpha_s(Q^2) \ln^2 N)^k$, the cross section is expected to have poles, and not cuts when $N = 0$, and indeed, a more detailed analysis reveals that the logarithmic behaviour of the cross section only arises through functions such as $\psi_0(N)$, which indeed has a simple pole at $N = 0$ even though $\psi_0(N) \sim \ln N$ as $N \to \infty$.

In Ref. [33] it was shown that indeed this approach leads to a very good approximation to the known NLO and NNLO expressions for the total cross section for Higgs production in gluon fusion with finite m_t (in particular, rather better than it would be found by simply expanding out the standard resummed result of Ref. [34]). An approximate expression for the N3LO correction to the cross section was then constructed.

The full N^{3}LO Higgs production cross section at the LHC at $\sqrt{s} = 8$ TeV, with $m_H = 125$ GeV was found to be (using the NNPDF2.1 PDF set with $\alpha_s(M_z) = 0.119$)

$$\begin{aligned}
\sigma^{\rm N^3LO}_{\rm approx}(\tau, m_H^2) &= \sigma^{(0)}(\tau, m_H^2) \left[\sum_{ij} \left(\delta_{ig}\delta_{jg} + \alpha_s K^{(1)}_{ij} + \alpha_s^2 K^{(2)}_{ij} \right) + \alpha_s^3 K^{(3)}_{gg,\rm approx} \right] \\
&= \left(22.61 \pm 0.27 + 0.91 \cdot 10^{-2} \bar{g}_{0,3}\right) \text{ pb} \qquad \text{for } \mu_R = m_H \\
&= \left(24.03 \pm 0.45 + 1.55 \cdot 10^{-2} \bar{g}_{0,3}\right) \text{ pb} \qquad \text{for } \mu_R = m_H/2,
\end{aligned} \tag{1.3}$$

where the error shown is an estimate of the uncertainty in the approximation procedure, and the coefficient $\bar{g}_{0,3}$ is unknown. The known perturbative behaviour of the coefficients $g_{0,i}$, which provide constant corrections to the cross section (i.e. neither logarithmically enhanced nor power-suppressed as $N \to \infty$) suggests that $\bar{g}_{0,3}$ is possibly of order ten. The renormalization scale dependence of the contribution from the gluon-gluon channel to the cross section is shown in Figure 1-8 for various choices of the collider energy (red band), and compared to the exact LO, NLO, and NNLO results, and also to the a different soft approximation and its collinear improvement (see below). Note that the factorization scale dependence of the result is known to be essentially negligible even at LO, more so at NLO and NNLO.

The main features of this approximate result are the following:

- The perturbative expansion converges quite slowly: in particular, it is clear that at each order the next-order result is not cointained within the range found varying the scale by a factor two about either m_H or $m_H/2$.
- The perturbative expansion converges better as the collider energy increases. The reason for this can be understood by computing the value of N which dominates the cross-section [35], which is fully determined by the collider energy and the Higgs mass, and then studying the perturbative behaviour of the cross section for the given value of N (see Figure 1-9).
- For all collider energies, the scale dependence is considerably reduced by the inclusion of the N^{3}LO corrections.
- The central prediction of Ref. [33], Eq. 1.3, amounts to a rather substantial correction, of order of 17% for $\mu_R = m_H$ at LHC 8 TeV.

- The N^{3}LO truncation of the resummed result of Ref. [34]) (also shown and labelled "N-soft" in Figure 1-8) together with its collinear improvement according to Ref. [36] (labelled "N-soft-coll") would predict a rather smaller correction to the NNLO result, of order of 6% for $\mu_R = m_H$.
- The whole NNLL correction to the NNLO result from Ref. [34] modifies the NNLO result by about 8%, 6% of which, as mentioned, comes from the N^{3}LO, and the remaining 2% or so from higher orders. This means that the resummation is perturbative in this region: it mostly amounts to a prediction for the N^{3}LO correction.
- The discrepancy between the prediction of a 6% correction N^{3}LO (expanding out the resummation of Ref. [34]) and a a 17% correction (using the approximation of Ref. [33]) is partly due to the choice of the value for the constant $\bar{g}_{0,3}$. In fact, using the value of the constant which is implicit in the resummed result of Ref. [34] reduces the N^{3}LO correction Eq. 1.3 from about 17% to about 12%. The remaning difference, which is thus by about a factor two for this scale choice, is due to the (allegedly more accurate) approximation of Ref. [33].
- The difference between the approximation of Ref. [33] and the expansion of the resummed result is mostly due to the fact that the soft approximation in Ref. [33] is designed to preserve the small N singularity structure. The explicit inclusion of the correct small N terms from the "BFKL" resummation has some effect in stabilizing somewhat the scale dependence at the very lowest edge $\mu_R/m_H < 0.1$ of the scale variation range of Figure 1-8, but it otherwise has a small impact.
- The scale dependence of the N^{3}LO result was also determined in Ref. [37] as a function of the value of the cross-section at the reference scale $\mu_R = m_H/2$. It was found that if this value is such that the scale dependence of the N^{3}LO is smaller than that of the NNLO, then the N^{3}LO is in the same ballpark as found in Ref. [33].

There are ongoing efforts to complete a full N^{3}LO calculation of the $gg \to H$ cross section, i.e. to provide the value of the coefficient $\bar{g}_{0,3}$ in equation 1.3. Given the slow convergence of the perturbative series for this process, a full calculation to this order may be necessary to achieve the needed theoretical precision for Higgs production, both for 14 TeV and for still higher energies.

1.4.7 Wishlist for higher order QCD and EW corrections

The Les Houches NLO wish list, consisting of calculations that were phenomenologically important for LHC physics, and were feasible but difficult to calculate at NLO in perturbative QCD, was started in 2005. After being incremented in 2007 and 2009 it was terminated in 2011. By 2011, every calculation on the wish list had been determined, and technology had advanced far enough that any reasonable multi-parton calculation could be carried out at NLO using semi-automated technology. In 2013, the NLO wish list was replaced by one at NNLO, the new calculational frontier; given the precision inherent at NNLO, many of the calculations on the list also involve the determination of electroweak corrections at NLO. The new wish list is shown in Tables 1-1, 1-2 and 1-3, giving the level to which the current calculation is known, and the level which is desired for full exploitation of physics at the LHC and higher energy hadron-hadron colliders. For the Higgs boson processes listed in Table 1-1 the improved calculations will enable more accurate extractions of Higgs couplings. The processes involving heavy quarks and jets, Table 1-2, will predominantly provide better extractions of pdfs. The vector boson processes given in Table 1-3 will be essential in investigating the precise nature of electroweak symmetry breaking – for instance by providing more accurate predictions for channels that are sensitive to vector boson scattering at high energy and to anomalous cubic and quartic gauge boson couplings.

Until recently, the start of the art for NNLO was the calculation of $2 \to 1$ processes. Within the last few years, several calculations of $2 \to 2$ processes have been completed. Indeed, the year 2013 has seen the completion of a number of landmark calculations at NNLO, namely the total cross section for top pair production [17] and first approximations of jet production [16] and the Higgs+jet process [30]. It is noteworthy that the wish list even contains $2 \to 3$ and $2 \to 4$ processes. Adding to the complexity is the need for the inclusion of decays for many of the massive final state particles. Given the recent progress in the field, it is difficult to speculate as to what length of time will be needed for the completion of this new list, but a period of 10 years may be a reasonable estimate.

Note that for many processes the higher order QCD and the higher order EWK corrections are currently known separately, while the desire is to have combined corrections, often at NNLO in QCD and NLO in EWK. One of the ambiguities in situations where the corrections are known separately is whether the two corrections are multiplicative or additive, i.e. whether the EWK corrections are affected by the (often) large QCD corrections. The degree to which the corrections are multiplicative or additive no doubt depends on the particular process and even on the observable within that process. The joint calculations posited here will resolve this ambiguity.

1.4.8 Sudakov logarithms

1.5 Higgs+jets uncertainties

ACKNOWLEDGEMENTS

J. Rojo is supported by a Marie Curie Intra–European Fellowship of the European Community's 7th Framework Programme under contract number PIEF-GA-2010-272515.

Process	known	desired	details
H	dσ @ NNLO QCD dσ @ NLO EW finite quark mass effects @ NLO	dσ @ NNNLO QCD + NLO EW MC@NNLO finite quark mass effects @ NNLO	H branching ratios and couplings
H + j	dσ @ NNLO QCD (g only) dσ @ NLO EW finite quark mass effects @ LO	dσ @ NNLO QCD + NLO EW finite quark mass effects @ NLO	H p_T
H + 2j	σ_{tot}(VBF) @ NNLO(DIS) QCD dσ(gg) @ NLO QCD dσ(VBF) @ NLO EW	dσ @ NNLO QCD + NLO EW	H couplings
H + V	dσ @ NNLO QCD dσ @ NLO EW	with $H \to \text{b}\bar{\text{b}}$ @ same accuracy	H couplings
t$\bar{\text{t}}$H	dσ(stable tops) @ NLO QCD	dσ(top decays) @ NLO QCD + NLO EW	top Yukawa coupling
HH	dσ @ LO QCD (full m_t dependence) dσ @ NLO QCD (infinite m_t limit)	dσ @ NLO QCD (full m_t dependence) dσ @ NNLO QCD (infinite m_t limit)	Higgs self coupling

Table 1-1. *Wishlist part 1 – Higgs (*V = W, Z*).*

Process	known	desired	details
t$\bar{\text{t}}$	σ_{tot} @ NNLO QCD dσ(top decays) @ NLO QCD dσ(stable tops) @ NLO EW	dσ(top decays) @ NNLO QCD + NLO EW	precision top/QCD, gluon PDF, effect of extra radiation at high rapidity, top asymmetries
t$\bar{\text{t}}$ + j	dσ(NWA top decays) @ NLO QCD	dσ(NWA top decays) @ NNLO QCD + NLO EW	precision top/QCD top asymmetries
single-top	dσ(NWA top decays) @ NLO QCD	dσ(NWA top decays) @ NNLO QCD (t channel)	precision top/QCD, V_{tb}
dijet	dσ @ NNLO QCD (g only) dσ @ NLO weak	dσ @ NNLO QCD + NLO EW	Obs.: incl. jets, dijet mass $\to$ PDF fits (gluon at high x) $\to \alpha_s$
3j	dσ @ NLO QCD	dσ @ NNLO QCD + NLO EW	Obs.: $R3/2$ or similar $\to \alpha_s$ at high scales dom. uncertainty: scales
γ + j	dσ @ NLO QCD dσ @ NLO EW	dσ @ NNLO QCD +NLO EW	gluon PDF γ + b for bottom PDF

Table 1-2. *Wishlist part 2 – jets and heavy quarks.*

Process	known	desired	details
V	dσ(lept. V decay) @ NNLO QCD dσ(lept. V decay) @ NLO EW	dσ(lept. V decay) @ NNNLO QCD + NLO EW MC@NNLO	precision EW, PDFs
V + j	dσ(lept. V decay) @ NLO QCD dσ(lept. V decay) @ NLO EW	dσ(lept. V decay) @ NNLO QCD + NLO EW	Z + j for gluon PDF W + c for strange PDF
V + jj	dσ(lept. V decay) @ NLO QCD	dσ(lept. V decay) @ NNLO QCD + NLO EW	study of systematics of H + jj final state
VV′	dσ(V decays) @ NLO QCD dσ(stable V) @ NLO EW	dσ(V decays) @ NNLO QCD + NLO EW	off-shell leptonic decays TGCs
gg → VV	dσ(V decays) @ LO QCD	dσ(V decays) @ NLO QCD	bkg. to $H \to VV$ TGCs
Vγ	dσ(V decay) @ NLO QCD dσ(PA, V decay) @ NLO EW	dσ(V decay) @ NNLO QCD + NLO EW	TGCs
Vb$\bar{\text{b}}$	dσ(lept. V decay) @ NLO QCD massive b	dσ(lept. V decay) @ NNLO QCD massless b	bkg. for VH → b$\bar{\text{b}}$
VV′γ	dσ(V decays) @ NLO QCD	dσ(V decays) @ NLO QCD + NLO EW	QGCs
VV′V″	dσ(V decays) @ NLO QCD	dσ(V decays) @ NLO QCD + NLO EW	QGCs, EWSB
VV′ + j	dσ(V decays) @ NLO QCD	dσ(V decays) @ NLO QCD + NLO EW	bkg. to H, BSM searches
VV′ + jj	dσ(V decays) @ NLO QCD	dσ(V decays) @ NLO QCD + NLO EW	QGCs, EWSB
$\gamma\gamma$	dσ @ NNLO QCD		bkg to $H \to \gamma\gamma$

Table 1-3. *Wishlist part 3 – EW gauge bosons* (V = W, Z).

References

[1] S. Forte and G. Watt, arXiv:1301.6754 [hep-ph].

[2] A. De Roeck and R. S. Thorne, Prog. Part. Nucl. Phys. **66**, 727 (2011) [arXiv:1103.0555 [hep-ph]].

[3] E. Perez and E. Rizvi, Rep. Prog. Phys. **76**, 046201 (2013) [arXiv:1208.1178 [hep-ex]].

[4] G. Bozzi, J. Rojo and A. Vicini, Phys. Rev. D **83**, 113008 (2011) [arXiv:1104.2056 [hep-ph]].

[5] S. Alekhin, J. Blumlein and S. Moch, Phys. Rev. D **86**, 054009 (2012) [arXiv:1202.2281 [hep-ph]].

[6] J. Gao, M. Guzzi, J. Huston, H. -L. Lai, Z. Li, P. Nadolsky, J. Pumplin and D. Stump *et al.*, arXiv:1302.6246 [hep-ph].

[7] V. Radescu [H1 and ZEUS Collaboration], PoS ICHEP **2010**, 168 (2010).

[8] A. M. Cooper-Sarkar [ZEUS and H1 Collaborations], PoS EPS **-HEP2011**, 320 (2011) [arXiv:1112.2107 [hep-ph]].

[9] A. D. Martin, W. J. Stirling, R. S. Thorne and G. Watt, Eur. Phys. J. C **63**, 189 (2009) [arXiv:0901.0002 [hep-ph]].

[10] R. D. Ball, V. Bertone, S. Carrazza, C. S. Deans, L. Del Debbio, S. Forte, A. Guffanti and N. P. Hartland *et al.*, Nucl. Phys. B **867**, 244 (2013) [arXiv:1207.1303 [hep-ph]].

[11] R. D. Ball, S. Carrazza, L. Del Debbio, S. Forte, J. Gao, N. Hartland, J. Huston and P. Nadolsky *et al.*, JHEP **1304**, 125 (2013) [arXiv:1211.5142 [hep-ph]].

[12] G. Aad *et al.* [ATLAS Collaboration], Phys. Rev. D **86**, 014022 (2012) [arXiv:1112.6297 [hep-ex]].

[13] S. Chatrchyan *et al.* [CMS Collaboration], Phys. Rev. D **87**, 112002 (2013) [arXiv:1212.6660 [hep-ex]].

[14] G. Aad *et al.* [ATLAS Collaboration], arXiv:1304.4739 [hep-ex].

[15] M. L. Mangano and J. Rojo, JHEP **1208**, 010 (2012) [arXiv:1206.3557 [hep-ph]].

[16] A. G. -D. Ridder, T. Gehrmann, E. W. N. Glover and J. Pires, Phys. Rev. Lett. **110**, 162003 (2013) [arXiv:1301.7310 [hep-ph]].

[17] M. Czakon, P. Fiedler and A. Mitov, arXiv:1303.6254 [hep-ph].

[18] M. Czakon, M. L. Mangano, A. Mitov and J. Rojo, arXiv:1303.7215 [hep-ph].

[19] R. D. Ball, V. Bertone, F. Cerutti, L. Del Debbio, S. Forte, A. Guffanti, J. I. Latorre and J. Rojo *et al.*, Nucl. Phys. B **849**, 296 (2011) [arXiv:1101.1300 [hep-ph]].

[20] R. D. Ball *et al.* [NNPDF Collaboration], Nucl. Phys. B **855**, 153 (2012) [arXiv:1107.2652 [hep-ph]].

[21] D. d'Enterria and J. Rojo, Nucl. Phys. B **860**, 311 (2012) [arXiv:1202.1762 [hep-ph]].

[22] L. Carminati, G. Costa, D. D'Enterria, I. Koletsou, G. Marchiori, J. Rojo, M. Stockton and F. Tartarelli, EPL **101**, 61002 (2013) [Europhys. Lett. **101**, 61002 (2013)] [arXiv:1212.5511 [hep-ph]].

[23] S. A. Malik and G. Watt, arXiv:1304.2424 [hep-ph].

[24] W. J. Stirling and E. Vryonidou, Phys. Rev. Lett. **109**, 082002 (2012) [arXiv:1203.6781 [hep-ph]].

[25] A. D. Martin, R. G. Roberts, W. J. Stirling and R. S. Thorne, Eur. Phys. J. C **39**, 155 (2005) [hep-ph/0411040].

[26] S. Carrazza, arXiv:1307.1131 [hep-ph].

[27] S. Carrazza, arXiv:1305.4179 [hep-ph].

[28] A. Bierweiler, T. Kasprzik, H. Kuhn and S. Uccirati, JHEP **1211**, 093 (2012) [arXiv:1208.3147 [hep-ph]].

[29] G. Ferrera, M. Grazzini and F. Tramontano, Phys. Rev. Lett. **107**, 152003 (2011) [arXiv:1107.1164 [hep-ph]].

[30] R. Boughezal, F. Caola, K. Melnikov, F. Petriello and M. Schulze, JHEP **1306**, 072 (2013) [arXiv:1302.6216 [hep-ph]].

[31] J. M. Campbell, R. K. Ellis and C. Williams, JHEP **1107**, 018 (2011) [arXiv:1105.0020 [hep-ph]].

[32] G. Aad *et al.* [ATLAS Collaboration], New J. Phys. **15**, 033038 (2013) [arXiv:1301.6872 [hep-ex]].

[33] R. D. Ball, M. Bonvini, S. Forte, S. Marzani and G. Ridolfi, Nucl. Phys. B **874**, 746 (2013) [arXiv:1303.3590 [hep-ph]].

[34] D. de Florian and M. Grazzini, Phys. Lett. B **718** (2012) 117 [arXiv:1206.4133 [hep-ph]].

[35] M. Bonvini, S. Forte and G. Ridolfi, Phys. Rev. Lett. **109**, 102002 (2012) [arXiv:1204.5473 [hep-ph]].

[36] S. Catani, D. de Florian, M. Grazzini and P. Nason, JHEP **0307** (2003) 028 [hep-ph/0306211].

[37] S. Buehler and A. Lazopoulos, arXiv:1306.2223 [hep-ph].

[38] N. Kidonakis and J. F. Owens, Phys. Rev. D **63**, 054019 (2001) [hep-ph/0007268].

[39] S. Frixione and B. R. Webber, JHEP **0206**, 029 (2002) [hep-ph/0204244].

[40] P. Nason, JHEP **0411**, 040 (2004) [hep-ph/0409146].

[41] S. Frixione, P. Nason and C. Oleari, JHEP **0711**, 070 (2007) [arXiv:0709.2092 [hep-ph]].

[42] S. Hoeche, F. Krauss, M. Schonherr and F. Siegert, JHEP **1304**, 027 (2013) [arXiv:1207.5030 [hep-ph]].

[43] R. Frederix and S. Frixione, JHEP **1212**, 061 (2012) [arXiv:1209.6215 [hep-ph]].

[44] S. Catani, F. Krauss, R. Kuhn and B. R. Webber, JHEP **0111**, 063 (2001) [hep-ph/0109231].

[45] L. Lonnblad, JHEP **0205**, 046 (2002) [hep-ph/0112284].

[46] M. L. Mangano, M. Moretti and R. Pittau, Nucl. Phys. B **632**, 343 (2002) [hep-ph/0108069].

[47] N. Lavesson and L. Lonnblad, JHEP **0812**, 070 (2008) [arXiv:0811.2912 [hep-ph]].

[48] L. Lnnblad and S. Prestel, JHEP **1303**, 166 (2013) [arXiv:1211.7278 [hep-ph]].

[49] S. Hoeche, F. Krauss, M. Schonherr and F. Siegert, Phys. Rev. Lett. **110**, 052001 (2013) [arXiv:1201.5882 [hep-ph]].

[50] S. Alioli, S. -O. Moch and P. Uwer, JHEP **1201**, 137 (2012) [arXiv:1110.5251 [hep-ph]].

[51] S. Hoeche, J. Huang, G. Luisoni, M. Schoenherr and J. Winter, arXiv:1306.2703 [hep-ph].

[52] Z. Nagy and D. E. Soper, JHEP **0709**, 114 (2007) [arXiv:0706.0017 [hep-ph]].

[53] S. Hoeche, F. Krauss, M. Schonherr and F. Siegert, JHEP **1209**, 049 (2012) [arXiv:1111.1220 [hep-ph]].

[54] S. Platzer and M. Sjodahl, JHEP **1207**, 042 (2012) [arXiv:1201.0260 [hep-ph]].

[55] S. Alioli, C. W. Bauer, C. J. Berggren, A. Hornig, F. J. Tackmann, C. K. Vermilion, J. R. Walsh and S. Zuberi, arXiv:1211.7049 [hep-ph].

[56] S. Alioli, C. W. Bauer, C. Berggren, A. Hornig, F. J. Tackmann, C. K. Vermilion, J. R. Walsh and S. Zuberi, arXiv:1305.5246 [hep-ph].

[57] J. R. Andersen and J. M. Smillie, JHEP **1001**, 039 (2010) [arXiv:0908.2786 [hep-ph]].

[58] J. R. Andersen and J. M. Smillie, JHEP **1106**, 010 (2011) [arXiv:1101.5394 [hep-ph]].

[59] J. R. Andersen, L. Lonnblad and J. M. Smillie, JHEP **1107**, 110 (2011) [arXiv:1104.1316 [hep-ph]].

[60] See web-page: `https://twiki.cern.ch/twiki/bin/view/LHCPhysics/HiggsEuropeanStrategy2012`.

[61] J. R. Andersen *et al.* [SM and NLO Multileg Working Group Collaboration], arXiv:1003.1241 [hep-ph].

[62] Z. Bern, L. J. Dixon, F. Febres Cordero, S. Hoeche, H. Ita, D. A. Kosower, D. Maitre and K. J. Ozeren, arXiv:1304.1253 [hep-ph].

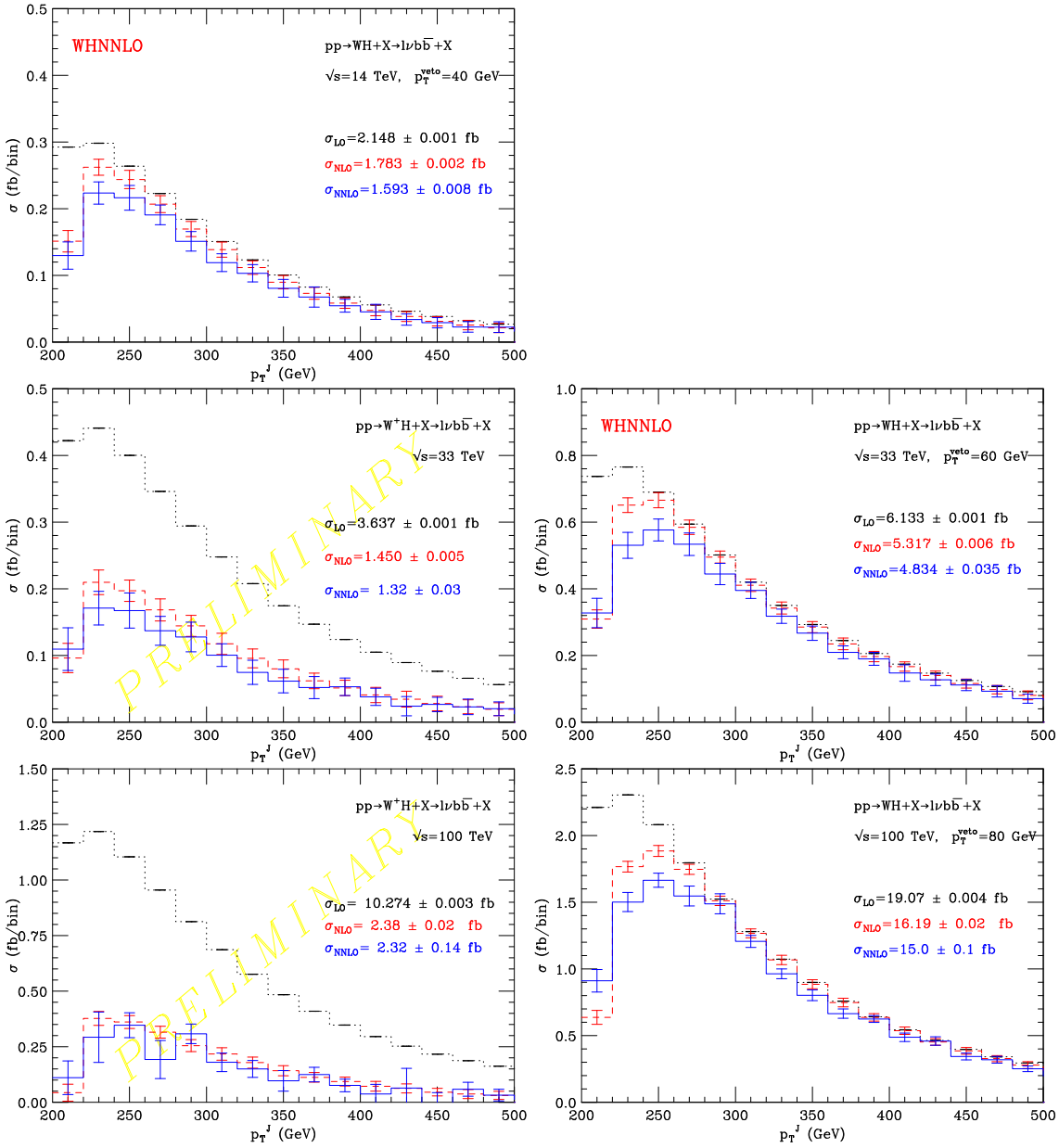

Figure 1-7. *The transverse momentum of the fat jet in WH production, at 14 TeV (top), 33 TeV (middle) and 100 TeV (bottom). In the left-hand column additional jets with transverse momenta above 40 GeV are vetoed, while in the right this veto is raised to 60 GeV at 33 TeV and 80 GeV at 100 TeV.*

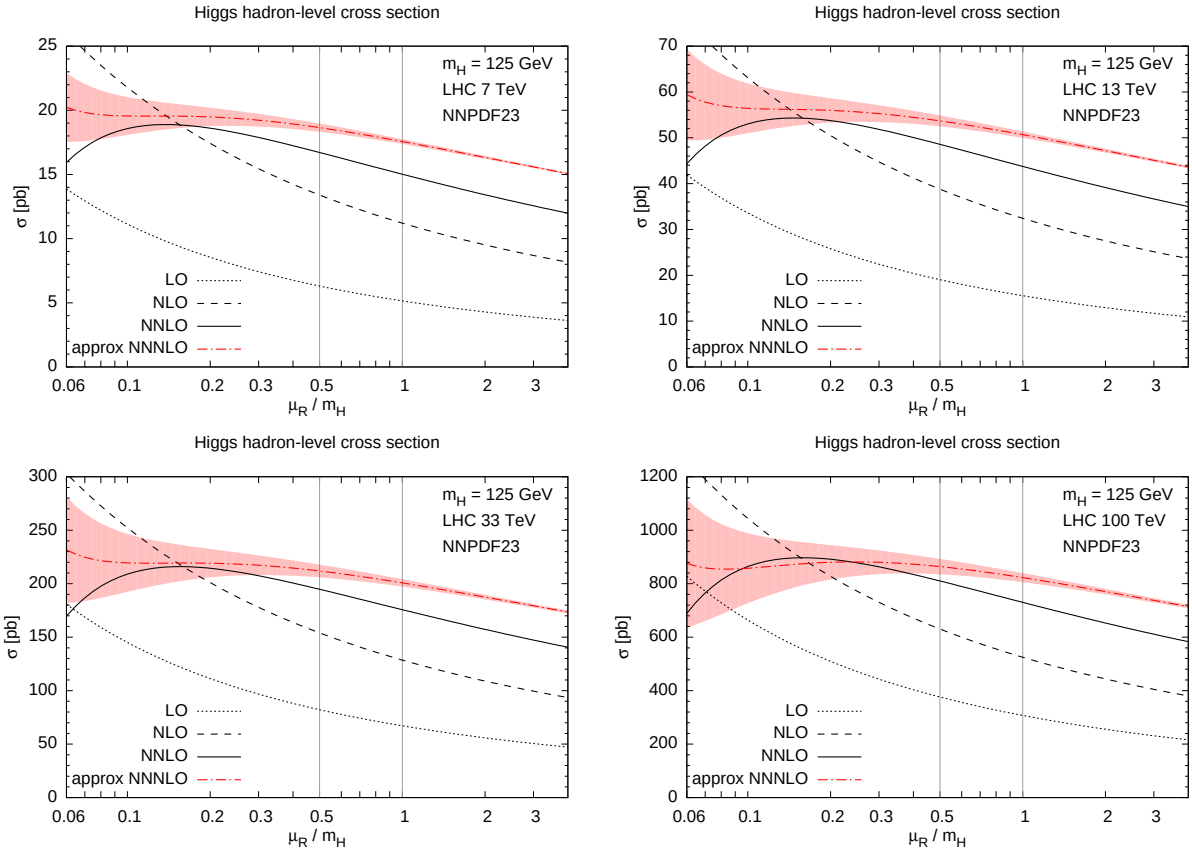

Figure 1-8. *Dependence on the renormalization scale of the LO, NLO, NNLO and approximate N^3LO contribution from the gluon-gluon channel to the total cross section for Higgs production at a proton-proton collider with four different values of the collider energy. The results shown are obtained using the NNPDF2.3 PDF set with $alpha_s(M_z) = 0.118$*

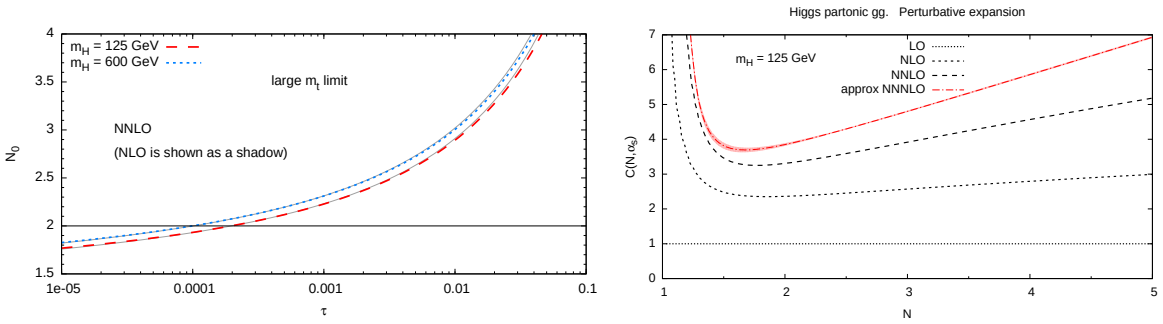

Figure 1-9. *Position of the saddle-point value of N which dominates the Mellin-space cross section for production of a 125 GeV Higgs boson in gluon fusion as a function of the collider energy (left), and perturbative expansion of the cross-section (right)*